Fast neutron time-encoded imaging with bubble masks

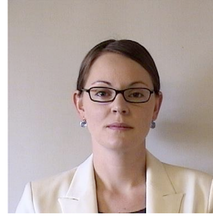

Erik Brubaker, James Brennan, Peter Marleau, Aaron Nowack, John Steele, **Melinda Sweany**, and Daniel Throckmorton

Sandia National Laboratories, 7011 East Ave, Livermore, CA 94550 (msweany@sandia.gov)

Motivation – real-time imaging of fast neutrons

Time-encoded imaging uses a modulated signal to reconstruct an image of a particle source: by introducing a known mask pattern of pin holes, a well-understood variation in the signal results for a given source distribution. For time-encoded imaging of fast neutrons, a mask pattern is constructed of a material such as high-density polyethylene, and the position of the mask elements with respect to a set of detectors is varied in time. We are exploring the possibility of using air bubbles propagating in hydrogenous liquids. Such a system would have the added ability of varying the mask pattern on the fly to account for different radiation environments:

- the open fraction of the mask pattern can be varied to optimize the signal to noise ratio
- the bubble size can be varied for high resolution imaging of a known source
- a known, strong source can be masked to search for nearby weak sources
- a background region known to contain no sources can be masked to increase the signal to noise ratio for unknown sources

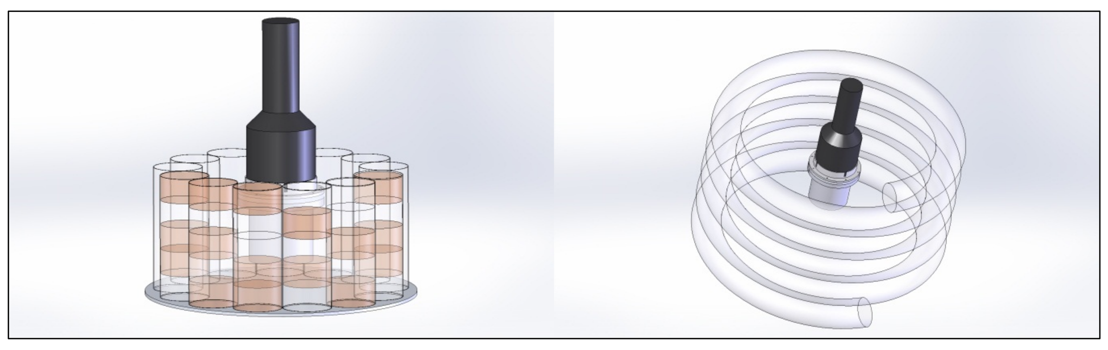

Figure 1: Two concepts of a time-encoded imaging system using air bubbles in hydrogenous materials

Methods – image reconstruction using MLEM

We use an iterative maximum-likelihood estimation maximization (MLEM) scheme [1] to reconstruct the true source distribution, broken into voxels indicated by the index *s*, based on the time-dependent shielding length *d(s,t)* between the source and detector. The likelihood is constructed from the Poisson probability of observing *n(t)* emitted events:

$$\mathcal{L} = \prod_{t=t_1,\dots,t_N} e^{-\lambda(t)} \frac{\lambda(t)^{n(t)}}{n(t)!},$$

where $\lambda(t)$ is the expected observation at time t. The estimate of the expected number from each voxel is:

$$\hat{\lambda}_{new}(s) = \hat{\lambda}_{old}(s) \sum_{t=t_1,\dots,t_N} \frac{n(t)\,\frac{e^{-d(s,t)/l}}{4\pi r(s)^2}}{\sum_{s'=1}^{S} \hat{\lambda}_{old}(s')\,\frac{e^{-d(s',t)/l}}{4\pi r(s')^2}},$$

where l is the neutron attenuation length of the fluid, and r(s) is the distance from the detector to voxel s.

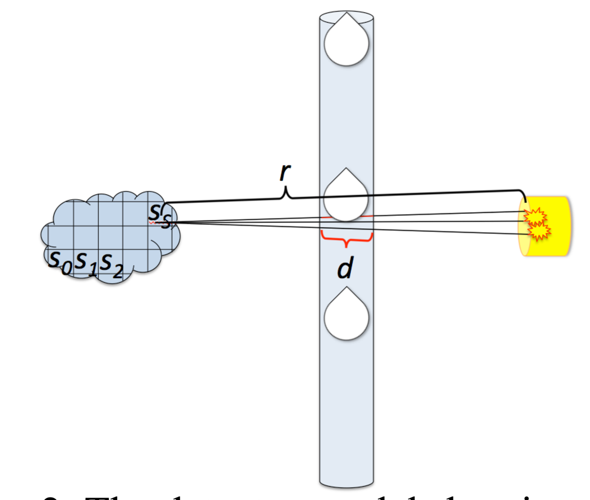

Figure 2: The detector model showing the source distribution with S source voxels, the tube attenuating the source distribution by $\sim e^{-d/l}$ (shown in red), and the detector.

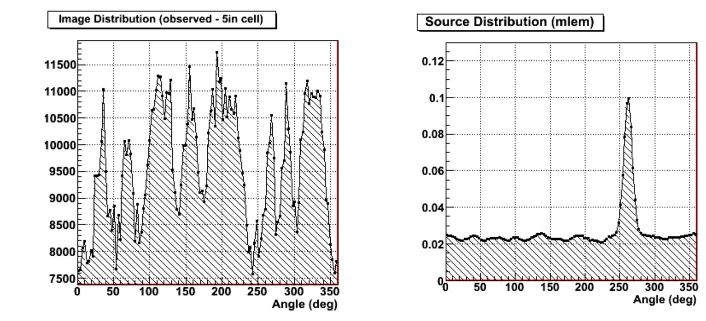

Figure 3: on the left is the neutron rate as a function of time for a prototype time-encoded imaging system, with the (MLEM) reconstructed source distribution shown on the right.

Simulation and Reconstruction – 2D masks

To reconstruct the neutron source image, the attenuation between the source and the detector needs to be determined in real time:

- The tube geometry is broken into voxels, and the attenuation per voxel is stored in memory for all possible source locations
- A random mask pattern is generated, propagated in time, and the attenuation when a bubble is absent is determined from the summed attenuation of the individual voxels with no bubble present
- The resulting 2D attenuation map is used to predict the source rate as a function of time for every possible source position
- MLEM is used to reconstruct the true source position

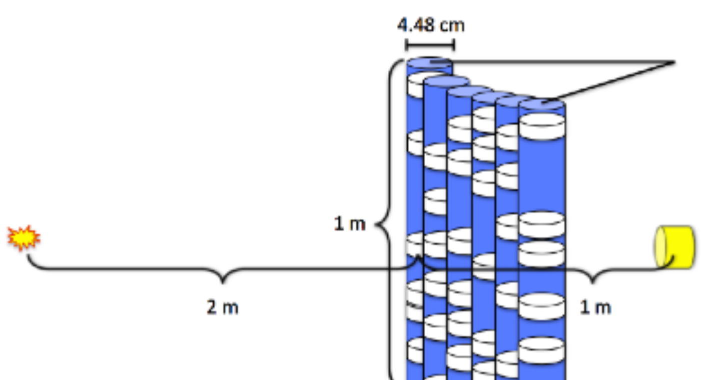

Figure 5: A 2D bubble mask with bubbles modeled as cylindrical voxels: the tubes are chosen to be one neutron attenuation length.

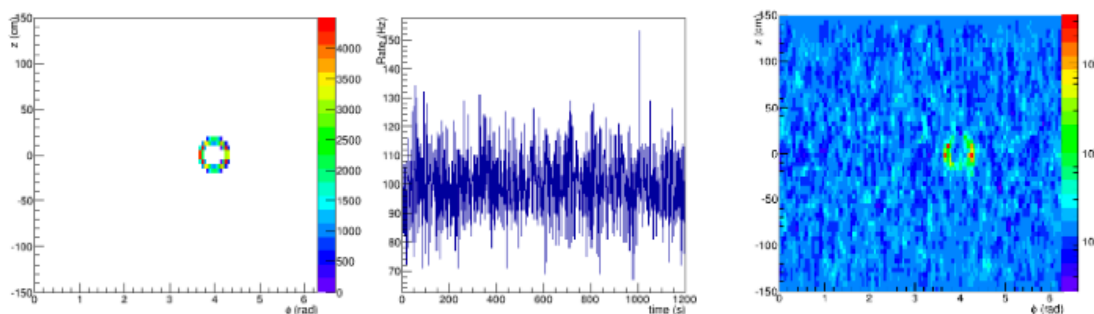

Figure 4: (left) The true source distribution with a rate of 10 Hz and no background. (center) The simulated event rate for a random mask of bubbles propagating at 10 cm/s and 50% open fraction. (right) The reconstructed source distribution after 20 minutes of acquisition time.

Detector development – bubble characteristics

In order to accurately model the neutron attenuation as a function of time, the shape of the bubble must have certain characteristics:

- reproducible
- shape that can be modeled easily
- maximum contrast between masked and open areas of the tube

Several approaches were tested, with varying results on the quality and consistency of the bubbles.

Figure 8: The effect of varying pulse duration and air pressure: on the left is a high-pressure short pulse, and on the right is a low-pressure long pulse

Figure 6: A two inch ID mask tube using a side inlet port

Figure 7: an example of the shearing and distortion introduced by the rigid side inlet design

Figure 9: Bubble shape in glycerine (left) and mineral oil (right)

Analysis – bubble tracking in real time

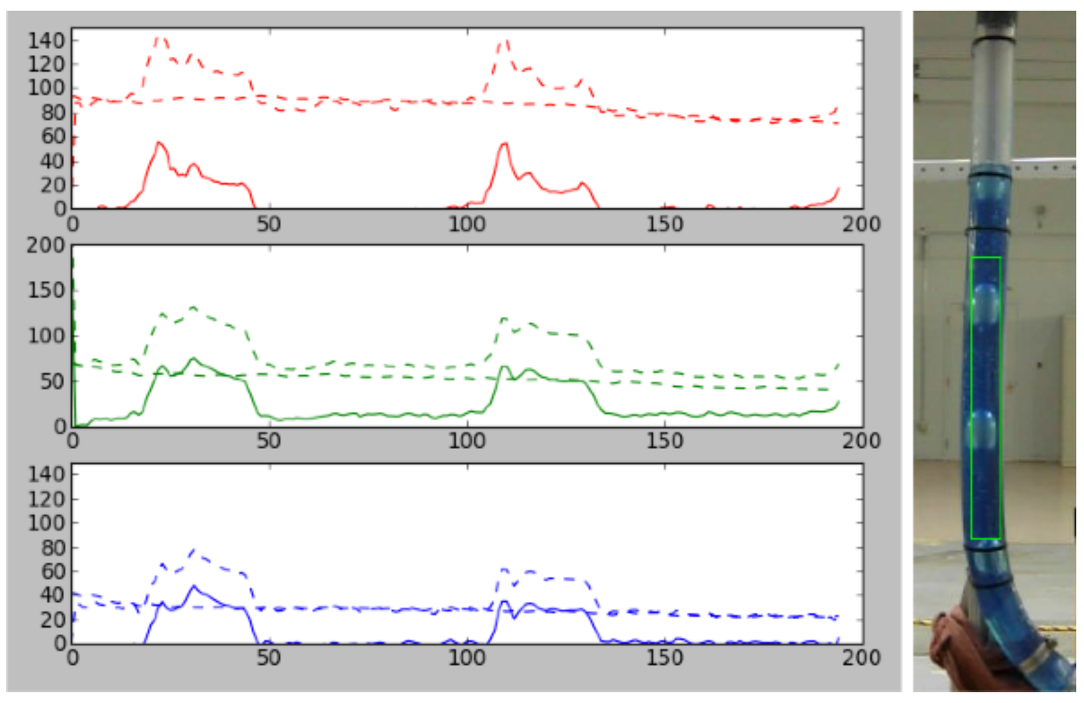

Figure 10: (left) The RGB pixel values averaged in the horizontal direction for one camera frame, indicating the location of bubbles in the region of interest, shown (right). The deviation from the baseline is the solid line, and the values with no bubbles present and with bubbles present are the dotted lines.

In order to reconstruct the source in real time, the bubbles in the tube are tracked with a USB camera. A bubble region of interest is defined in the field of view of the camera, and the software OpenCV [2] is used to manipulate the video frames of the camera. Pixel values are averaged horizontally, and a threshold over the baseline is used to determine the location of bubbles in a given frame. The empty tube voxels are passed to the reconstruction algorithm, where the stored attenuation is used to determine the source configuration and strength that yields the measured rate.

Results – 1D mask pattern

Figure 11: The 1D bubble mask setup in the lab, with glycerol as the mask medium. The detector is 2x2 inch cylindrical tube of liquid scintillator.

Two equal strength ^{252}Cf sources were placed at two z-positions along the tube. Pulse-shape discrimination is used to pick out neutron events. The source position reconstruction for a random bubble mask pattern is shown in Figure 11.

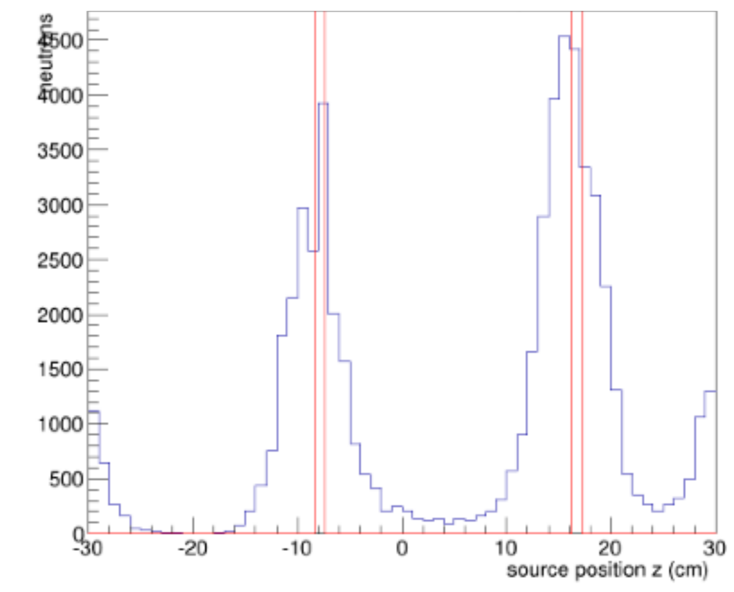

Figure 12: The true (red) and reconstructed (blue) source positions for a 5 minute run (above) and 60 minute run (below).

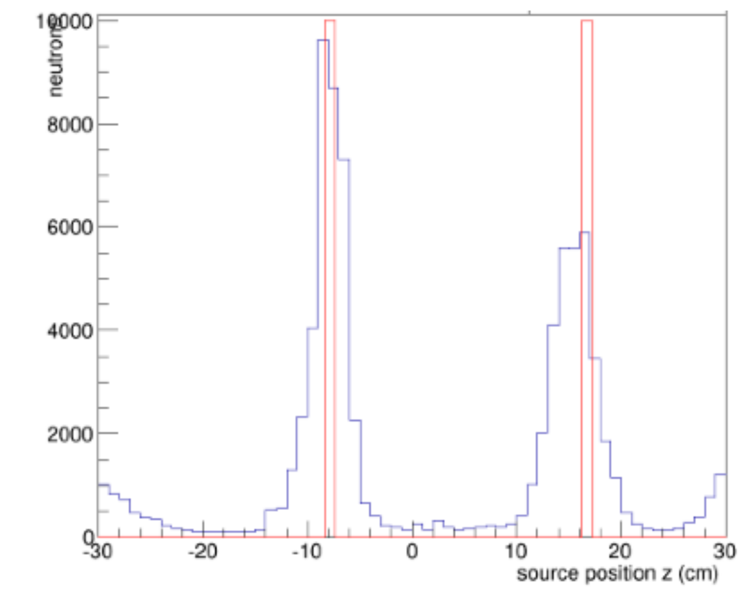

References:

[1] L. A. Shepp and Y. Vardi. *IEEE Transactions on Medical Imaging* **1** (1982) 113-122

[2] G. Bradski. "The OpenCV Library" *Dr. Dobb's Journal of Software Tools* (2000)

This work was supported by Laboratory Directed Research and Development (LDRD) at Sandia National Laboratories. Sandia National Laboratories is a multi-program laboratory managed and operated by Sandia Corporation, a wholly owned subsidiary of Lockheed Martin Corporation, for the U.S. Department of Energy's National Nuclear Security Administration under Contract DE-AC04-94AL85000. (2014-4168C)